Journal of Thermodynamics & Catalysis
ISSN: 2157-7544

Vivier et al., J Thermodyn Catal 2012, 3:2
DOI: 10.4172/2157-7544.1000114

Research Article Open Access

Thermodynamics of CO_2-MDEA using eNRTL with Differential Evolution Algorithm

Jacques Vivier, Saeid Kamalpour and Amine Mehablia*

CNRS-IAARC - Centre National de la Recherche Scientifique 3, rue Michel-Ange 75794 Paris cedex 16 - France

Abstract

Carbon dioxide capture by absorption with aqueous alkanolamines is considered an important technology to reduce CO_2 emissions and to help alleviate global climate change. To understand more the thermodynamics of some of the CO_2-Amines, the NRTL electrolyte model has been used to simulate the behavior of carbon dioxide absorption by MDEA. VLE, heat capacity and excess enthalpy data have been used to regress the interactions parameters of the model by minimizing the objective function using differential evolution algorithm (DE), an evolutionary computational technique.

Differential Evolution algorithm (DE) is compared with other techniques such as annealing (SA) and Levenberg–Marquardt (LM) using one set of experimental data for MDEA-H_2O system. The results show that its standard deviations are lower than those of SA and LM algorithms.

Keywords: CO_2; MDEA; Modeling; NRTL; Differential evolution

Introduction

In the field of evolutionary algorithm, Differential Evolution (DE) has gained a great focus due to its strong global optimization capability and simple implementation. Differential evolution (DE) is an efficient and powerful population-based stochastic search technique for solving optimization problems over continuous space, which had been widely applied in many scientific and engineering fields. The carbon dioxide capture has been the focus in this application.

Differential Evolution (DE) algorithm is a new heuristic approach mainly having three advantages; finding the true global minimum regardless of the initial parameter values, fast convergence and using few control parameters. DE algorithm is a population based algorithm like genetic algorithms using similar operators; crossover, mutation and selection. However, the success of DE in solving a specific problem crucially depends on appropriately choosing trial vector generation strategies and their associated control parameter values. Employing a trial-and-error scheme to search for the most suitable strategy and its associated parameter settings requires high computational costs. Moreover, at different stages of evolution, different strategies coupled with different parameter settings may be required in order to achieve the best performance. The NRTL-electrolyte model has been used for CO_2 absorption by MDEA where DE has been applied to have a better optimization of the model.

Scalable simulation, design, and optimization of the CO_2 capture processes start with modeling of the thermodynamic properties, specifically vapor-liquid equilibrium (VLE) and chemical reaction equilibrium, as well as calorimetric properties. Accurate modeling of thermodynamic properties requires availability of reliable experimental data. For the rational gas treating processes the knowledge of VLE of the acid gas over alkanolamine solution is required besides the knowledge of mass transfer and kinetics. The major problem concerning the VLE measurements of aqueous alkanolamine-acid gas systems, in general, is that lack of consistency and regularity in the numerous published values.

Excess Gibbs energy-based activity coefficient models provide a practical and rigorous thermodynamic framework to model thermodynamic properties of aqueous electrolyte systems, including aqueous alkanolamine systems for CO_2 capture [1,2] Austgen et al. [3] and Posey [4] applied the electrolyte NRTL model [5-7] to correlate CO_2 solubility in aqueous MDEA solution and other aqueous alkanolamines.

Kuranov et al. [8], and Kamps et al. [9], used Pitzer's equation correlate the VLE data of the MDEA-H_2O-CO_2 system. Faramarzi et al. [10], used the extended UNIQUAC model [11] to represent VLE for CO_2 absorption in aqueous MDEA, MEA, and mixtures of the two alkanolamines. Arcis et al. [12] also fitted the VLE data with Pitzer's equation and used the thermodynamic model to estimate the enthalpy of solution of CO_2 in aqueous MDEA.

In this work, we used the electrolyte NRTL model as the thermodynamic framework to correlate experimental data for CO_2 absorption in aqueous MDEA solution. The present work requires solving multivariable optimization problem to determine the interaction parameters of the developed VLE model. In the present paper, DE algorithms [13] have been used for estimation of interaction parameters of the VLE model over a wide range of temperature, CO_2 partial pressure, and amine concentration range. Differential evaluation (DE) is a generic name for a group of algorithms, which is based on the principles of GA (Genetic Algorithm) but have some inherent advantages over GA, like its simple structure, ease of use, speed, and robustness.

We expand the scope of the work of Austgen et al. [3] and Posey [4] to cover all thermodynamic properties. Much new data for

***Corresponding author:** Amine Mehablia, CNRS-IAARC - Centre National de la Recherche Scientifique 3, rue Michel-Ange 75794 Paris cedex 16 – France, E-mail: amine.mehablia@iaarc.eu

Received April 23, 2012; **Accepted** April 23, 2012; **Published** April 28, 2012

Citation: Vivier J, Kamalpour S, Mehablia A (2012) Thermodynamics of CO_2-MDEA using eNRTL with Differential Evolution Algorithm. J Thermodyn Catal 3:114. doi:10.4172/2157-7544.1000114

thermodynamic properties and calorimetric properties have become available in recent years, and they cover wider ranges of temperature, pressure, MDEA concentration and CO_2 loading. The binary NRTL parameters for MDEA-water binary are regressed from the binary VLE, excess enthalpy, and heat capacity data. The binary NRTL parameters for water-electrolyte pairs and MDEA-electrolyte pairs and the standard-state properties of protonated MDEA ion are obtained by fitting to the ternary VLE, heat of absorption, heat capacity and NMR spectroscopic data.

With the use of the electrolyte NRTL model for the liquid-phase activity coefficients, the PC SAFT [14,15] equation of state (EOS) is used for its ability to model vapor-phase fugacity coefficients at high pressures, which is an important consideration for modeling CO_2 compression, where its parameters used in Zhang and Chen [16], Gross and Sadowki [15] and AspendataBank [16]. The PC-SAFT parameters used in this model are given in Table 1.

PC-SAFT is described more in detail by Goss and Sadowsky [14].

Thermodynamic Framework

Chemical and phase equilibrium

Carbon dioxide solubility in aqueous amine solutions is determined by both its physical solubility and the chemical equilibrium for the aqueous phase reactions among CO_2, water, and amines. The equilibrium of CO_2 in vapor and liquid phases is expressed in the following chemical equilibrium

$$CO_2(v) \leftrightarrow CO_2(l) \tag{1}$$

where it an been expressed in Henry's law by the following formula

$$Py_{CO_2}\varnothing_{CO_2} = H_{CO_2}x_{CO_2}\gamma^{*}_{CO_2} \tag{2}$$

where $\varnothing_{CO2}$ the CO_2 fugacity coefficient in the vapor phase, H_{CO2} the Henry's law constant of CO_2 in the mixed solvent of water and amine, $\gamma^{*}_{CO_2}$ the unsymmetrical activity coefficient of CO_2 in the mixed solvent of water and amine, P is the system pressure, y_{CO_2} the mole fraction of CO_2 in the vapor phase, and x_{CO_2} the equilibrium CO_2 mole fraction in the liquid phase.

And, the Henry's constant in the mixed solvent can be calculated from those of the pure solvents [17]:

$$\ln\left(\frac{H_i}{\gamma_i^{\infty}}\right) = \sum_A x_A \ln\left(\frac{H_{iA}}{\gamma_{iA}^{\infty}}\right) \tag{3}$$

H_{iA} The Henry's constant of supercritical component i in pure solvent A, the infinite dilution activity coefficient of supercritical component i in the mixed solvent, γ_{iA}^{∞} the infinite dilution activity coefficient of supercritical component i in pure solvent A, and x_A the mole fraction of solvent A, and H_i is the Henry's constant of supercritical component in the mixed solvent.

	MDEA	H_2O	CO_2
Source	16	14, 15	16
Segment number, parameter, m	3.3044	1.0656	2.5692
Segment energy Parameter, ε	237.44°K	366.51°K	152.10°K
Segment size Parameter, σ	3.5975Å	3.0007Å	2.5637 Å
Association energy Parameter, ε^{AB}	3709.9°K	2500.7°K	0°K
k^{AB}	0.066454 A^3	0.034868 A^3	0A^3

Table 1: For PC-SAFT Equation of State.

w_A is used instead of x_A in Equation 3 to weigh the contributions from different solvent [16]. The parameter w_A is calculated using Equation 4:

$$w_A = \frac{x_A(V_{iA}^{\infty})^{2/3}}{\sum_B x_B(V_{iA}^{\infty})^{2/3}} \tag{4}$$

V_{iA}^{∞} represents the partial molar volume of supercritical component i at infinite dilution in pure solvent A, calculated from the Brelvi-O'Connell model [18] with the characteristic volume for the solute ($V_{CO_2}^{BO}$) and solvent (V_S^{BO}).

The correlation of the characteristic volume for the Brelvi-O'Connell model (V_i^{BO}) is given as follows:

$$V_i^{BO} = v_{1,i} + v_{2,i}T \tag{5}$$

Here, the critical volume, $v_{n,i}$, was used as the characteristic volume for MDEA Zhang and Chen [15] , for CO_2 from Yan and Chen [5] and for H_2O from Brelvi and O'Connell [18].

The correlation for Henry's constant is given as follows:

$$\ln H_{ij} = a_{ij} + b_{ij}/\ln T + c_{ij}\ln T + d_{ij}T \tag{6}$$

These parameters can be found in Yan and Chen [19] for $CO_{2\,(solute)}$-$H_2O_{(solvent)}$ and in Zhang and Chen [15] for $CO_{2(solute)}$-$MDEA_{(solvent)}$

Aqueous-phase chemical equilibrium

The processes discussed involve both chemical equilibria and multi-component phase equilibria. The liquid phase comprises both molecular species and ionic species, which makes the modelling non-trivial. The chemical reactions taking place in the liquid phase for MDEA-CO_2-H_2O can be expressed as:

Water ionisation

$$2H_2O \leftrightarrow H_3O^{+} + OH^{-} \tag{7}$$

Dissociation of carbon dioxide

$$CO_2 + 2H_2O \leftrightarrow H_3O^{+} + HCO_3^{-}\sum \tag{8}$$

Dissociation of bicarbonate

$$HCO_3^{-} + H_2O \leftrightarrow H_3O^{+} + CO_3^{2-} \tag{9}$$

Dissociation of protonated amine

$$MDEAH^{+} + H_2O \leftrightarrow H_3O^{+} + MDEA \tag{10}$$

The equilibrium constants of the chemical reactions (8-11) can be expressed as follows:

$$K = \prod(\gamma_i x_i)^{\vartheta i} \tag{11}$$

Or another form of the equilibrium constant, K_j, of reaction j, can take place using the reference-state Gibbs free energies, G_j^o, of the participating components

$$-RT\ln K_j = \Delta G_j^0(T) \quad (12)$$

For the aqueous phase reactions, the reference states chosen are pure liquid for the solvents (water and MDEA), and aqueous phase infinite dilution for the solutes (ionic and molecular).

The thermodynamic expression for equilibrium partial pressure of CO_2 in aqueous MDEA solutions is as follows[3]:

$$P_{CO2} = \frac{H_{CO2}K_2 x_{MDEAH+}\gamma_{MDEAH+}x_{HCO3-}\gamma_{HCO3-}}{K_1 x_{H2O}x_{MDEA}\gamma_{H2O}\gamma_{MDEA}} \quad (13)$$

where, x_{ns} are the liquid phase mole fractions of the components, based on true molecular or ionic species at equilibrium.

The calculation of the concentration for each component at equilibrium is as follows:

$$C_{MDEAH+} = C_{HCO_3^-} = C^0_{MDEA}\alpha_{CO2} \quad (14)$$

$$C_{MDEA} = C^0_{MDEA}(1-\alpha) \quad (15)$$

Activity coefficients γ_i, (based on mole fraction scale) for different species present in the liquid phase are calculated from NRTL model.

Henry's law constants for CO_2 with water and for CO_2 with MDEA are required. Because of the reaction between CO_2 and amines, it is impossible to get its solubility in amines or MDEA. So for the prediction of the physical solubility in aqueous MDEA, the CO_2 –N_2O analogy is widely accepted in the literature [15]. This theory is based on the fact that CO_2 and N_2O are rather similar molecules. The only difference between the molecules is, that N_2O does not chemically (only physically) dissolve in aqueous MDEA. According to the CO_2 – N_2O analogy the Henry's constant (physically dissolved)

So a similar molecular structure of CO_2 is chosen, N_2O, to derive its physical solubility in amines, where their Henry constants are related according to Equation 5.

$$\frac{H_{CO_2,MDEA}}{H_{N_2O,MDEA}} = \frac{H_{CO_2,water}}{H_{N_2O,water}} \quad (16)$$

The solubility of N_2O in pure MDEA was reported by Wang et al. [20]. And based on the work of Versteef and van Swaiij [21], we obtained the solubilities of CO_2 and N_2O in water. Then we can use Equation 7 to determine $H_{CO2,MDEA}$ and its parameters.

Model and data used

The Gibbs free energy of solvent s, G_s, is calculated from the ideal gas Gibbs free energy of solvent *s*, G_s^{ig}, and the Gibbs free energy departure, $G_s^{ig\to l}$, from ideal gas to liquid at temperature T.

$$G_s(T) = G_s^{ig}(T) + \Delta G_s^{ig\to l}(T) \quad (17)$$

The ideal gas Gibbs free energy of solvent s, G_s^{ig}, is calculated from the ideal gas Gibbs free energy of formation of solvent s at 298.15°K, $\Delta_f G^{ig}_{s,298.15}$, the ideal gas enthalpy of formation of solvent s at 298.15°K, $\Delta_f H^{ig}_{s,298.15}$, and the ideal gas heat capacity of solvent *s*, $C^{ig}_{p,s}o$.

$$G_s^{ig}(T) = \Delta_f H^{ig}_{s,298.15} + \int_{298.15}^{T} C^{ig}_{p,s}dT - T^*\left(\frac{\Delta_f H^{ig}_{s,298.15} - \Delta_f G^{ig}_{s,298.15}}{298.15} + \int_{298.15}^{T}\frac{C^{ig}_{p,s}}{T}dT\right) \quad (18)$$

The reference-state properties $\Delta_f G^{ig}_{s,298.15}$ and $\Delta_f H^{ig}_{s,298.15}$ are obtained from Aspen Databank [16] and regressed from Wagman et al. [22] and Zhang and Chen [15].

The correlation for the ideal gas heat capacity is given as follows:

$$C_p^{ig} = C_{1i} + C_{2i}T + C_{3i}T^2 + \ldots C_{6i}T^5 where C_{7i} < T < C_{8i} \quad (19)$$

The reference-state properties $\Delta_f G^{ig}_{s,298.15}$ and $\Delta_f H^{ig}_{s,298.15}$ can be obtained from Aspen Databank [16], Wagman et al. [22], and Zhang and Chen [15]. The ideal heat capacities are obtained from Aspen Databank [16] and Zhang and Chen [15]. For water, The Gibbs free energy departure function is obtained from ASME steam tables. For MDEA, the departure function is calculated from the PC-SAFT EOS.

For molecular solute CO_2, the Gibbs free energy in aqueous phase infinite dilution is calculated from Henry's law:

$$G_i^{\infty,aq}(T) = \Delta_f G_i^{ig}(T) + RT\ln\left(\frac{H_{i,w}}{P^{ref}}\right) \quad (20)$$

Where $G_i^{\infty,aq}(T)$ is the mole fraction scale aqueous-phase infinite dilution Gibbs free energy of solute i at temperature T, $\Delta_f G_i^{ig}(T)$ the ideal gas Gibbs free energy of formation of solute i at temperature T, $H_{i,w}$ the Henry's constant of solute i in water, and P^{ref} the reference pressure.

For ionic species, the Gibbs free energy in aqueous-phase infinite dilution is calculated from the Gibbs free energy of formation in aqueous-phase infinite dilution at 298.15°K, the enthalpy of formation in aqueous-phase infinite dilution at 298.15°K, and the heat capacity in aqueous-phase infinite dilution

$$G_i^{\infty,aq}(T) = \Delta_f H^{\infty,aq}_{i,291.15} + \int_{298.15}^{T} C^{\infty,aq}_{p,i}dT - T^*\left(\frac{\Delta_f H^{\infty,aq}_{i,291.15} - \Delta_f G^{\infty,aq}_{i,2918.15}}{298.15} + \int_{298.15}^{T}\frac{C^{\infty,aq}_{p,i}}{T}dT\right) + RT\ln\left(\frac{1000}{M_w}\right) \quad (21)$$

Here, $G_i^{\infty,aq}(T)$ is the mole fraction scale aqueous-phase infinite dilution Gibbs free energy of solute i at temperature T, $\Delta_f G^{\infty,aq}_{i,298.15}$ the molality scale aqueous-phase infinite dilution Gibbs free energy of formation of solute i at 298.15°K, $\Delta_f H^{\infty,aq}_{i,291.15}$ the aqueous phase infinite dilution enthalpy of formation of solute *i* at 298.15°K, and $C^{\infty,aq}_{p,i}$ the aqueous-phase infinite dilution heat capacity of solute i. The term $RT\ln(1000/M_w)$ is added because $\Delta_f G^{\infty,aq}_{i,2918.15}$, as reported in the literature, is based on molality concentration scale while $G_i^{\infty,aq}$ is based on mole fraction scale.

The standard-state properties $G_i^{\infty,aq}$, $\Delta_f H^{\infty,aq}_{i,291.15}$ and $\Delta_f G^{\infty,aq}_{i,298.15}$ are obtained from Aspen Databank [16] and Criss and Gobble [23] for most ionic species. For $MDEAH^+$, they are calculated from the equilibrium constant [24].

Heat of absorption and heat capacity

The CO_2 heat of absorption in aqueous MDEA solutions can be derived from an enthalpy balance of the absorption process:

$$\Delta H_{abs} = n_{Final}H^l Final - n_I initial H^l lntial - n_{CO_2}H^g_{CO_2})/n_{(CO_2)} \quad (22)$$

Where ΔH_{abs}, Heat of absorption per mole of CO_2, H^l_{final}, Molar enthalpy of the final solution, H^l_{Intial}, Molar enthalpy of the initial solution, $H^g_{CO_2}$, Molar enthalpy of gaseous CO_2 absorbed, n_{final}, Number of moles of the final solution, $n_{Initial}$, Number of moles of the initial solution and n_{CO_2}, Number of moles of CO_2 absorbed.

To calculate the heat of absorption, enthalpy calculations for the final and initial MDEA-CO_2-H_2O system and for gaseous CO_2 are required. The heat capacity of MDEA-CO_2-H_2O system can be calculated from the temperature derivative of enthalpy.

We use the following equation for liquid enthalpy

$$H^l = x_w H^l_w + x_s H^l_s + \sum_i x_i H^{\infty,aq}_i + H^{ex} \quad (23)$$

Here, H^l is the molal enthalpy of the liquid mixture, H^l_w the molar enthalpy of liquid water, H^l_s the molar enthalpy of liquid nonaqueous solvent s, $H^{\infty,aq}_i$ the molar enthalpy of solute a (molecular or ionic) in aqueous-phase infinite dilution, and H^{ex} the molar excess enthalpy. The terms x_w, x_s and x_i represent the mole fractions of water, nonaqueous solvent s, and solute *i* respectively.

The liquid enthalpy for pure water is calculated from the ideal gas model and ASME Tables EOS for enthalpy departure:

$$H^l_w(T) = \Delta_f H^{ig}_{w,298.15} + \int_{298.15}^{T} C^{ig}_{p,w} dT + \Delta H^{ig\to l}_w(T,p) \quad (24)$$

where $H^l_w(T)$ is the liquid enthalpy of water at temperature T, $\Delta_f H^{ig}_{w,298.15}$ the ideal gas enthalpy of formation of water at 298.15°K, $C^{ig}_{p,w}$ the ideal-gas heat capacity of water, and $\Delta H^{ig\to l}_w(T,p)$ the enthalpy departure calculated from the ASME Steam Tables EOS.

Liquid enthalpy of the nonaqueous solvent s is calculated from the ideal-gas enthalpy of formation at 298.15°K, the ideal gas heat capacity, the vapor enthalpy departure, and the heat of vaporization:

$$H^l_w(T) = \Delta_f H^{ig}_{w,298.15} + \int_{298.15}^{T} C^{ig}_{p,s} dT + \Delta H^v_s(T,p) - \Delta_{vap} H_s(T) \quad (25)$$

Here, $H^l_s(T)$ is the liquid enthalpy of solvent s at temperature T, $\Delta_f H^{ig}_{s,298.15}$ the ideal-gas enthalpy of formation of solvent s at 298.15°K, $C^{ig}_{p,s}$ the ideal-gas heat capacity of solvent s, $\Delta H^v_s(T,p)$ the vapor enthalpy departure of solvent s, and $\Delta_{vap} H_s(T)$ the heat of vaporization of solvent s.

The PC-SAFT EOS is used for the vapor enthalpy departure and the DIPPR heat of vaporization correlation is used for the heat of vaporization. The DIPPR equation is:

$$\Delta_{vap} H_i = C_{(1i)}(1 - T_r i)^Z \quad (26)$$

Where $Z = C_{2i} + C_{3i} T_{ri} + C_{4i} T^2_{ri} + C_{5i} T^3_{ri}$ and $T_{ri} = T / T_{ci}$ (T_{ci} is the critical temperature of component i in K). The T_{ci} of MDEA is obtained from Von Niederhausern et al. [25]. The correlation parameters are obtained from Zhang and Chen [15].

Heat of vaporization of MDEA, $P^{\star,l}_{MDEA}$, calculated from the vapor Pressure (Antoine Equation, $P^{\star,l}_{MDEA}$) using the Clausius-Clapeyron equation,

$$\ln P^{\star,l}_{MDEA} = C_1 + \frac{C_2}{T} + C_3 \ln T + \frac{C_4}{T^2} \quad (27)$$

The parameters above, C_n, are regressed using the vapor pressure data [25-27].

The enthalpies of ionic solutes in aqueous phase infinite dilution are calculated from the enthalpy of formation at 298.15°K in aqueous-phase infinite dilution and the heat capacity in aqueous-phase infinite dilution:

$$H^{\infty,aq}_i(T) = \Delta_f H^{\infty,aq}_{i,298.15} + \int_{298.15}^{T} C^{\infty,aq}_{p,i} dT \quad (28)$$

where $H^{\infty,aq(T)}_i$ is the enthalpy of solute i in aqueous-phase infinite dilution at temperature T, $\Delta_f H^{\infty,aq}_{i,298.15}$ the enthalpy of formation of solute i in aqueous-phase infinite dilution at 298.15°K, and $C^{\infty,aq}_{p,i}$ the heat capacity of solute *i* in aqueous-phase infinite dilution.

In this study, $\Delta_f Hi^{\infty,aq}{}_{298,15})$ and $C^{\infty,aq}_{p,i}$ for $MDEAH^+$ are determined by fitting to the experimental phase equilibrium data, the heat of solution data, and the speciation data, together with molality scale Gibbs free energy of formation at 298.15°K, $\Delta_f G^{\infty,aq}_{i,298.15}$, and NRTL interaction parameters.

The enthalpies of molecular solutes in aqueous phase infinite dilution are calculated from Henry's law:

$$H^{\infty,aq}_i(T) = \Delta_f H^{ig}_i(T) - RT^2 \left(\frac{\partial \ln H_{i,w}}{\partial T} \right) \quad (29)$$

Where $\Delta_f H^{ig}_i(T)$ is the ideal gas enthalpy of formation of solute I, temperature T, H_{iw} Henry's constant of solute *i* in water. Excess enthalpy, $H^e x$ is calculated from the activity coefficient model, NRTL in this case.

The eNRTL model

The electrolyte NRTL model consists of three contributions. The first contribution is the long-range contribution represented by the Pitzer-Debye-Hückel expression, which accounts for the contribution due to the electrostatic forces among all ions. The second contribution is an ion-reference-state-transfer contribution represented by the Born expression. In the electrolyte NRTL model, the reference state for ionic species is always infinitely dilute state in water even when there are mixed solvents. The Born expression accounts for the change of the Gibbs energy associated with moving ionic species from a mixed-solvent infinitely dilute state to an aqueous infinitely dilute state. The Born expression drops out if water is the sole solvent in the electrolyte system. The third contribution is a short-range contribution represented by the local composition electrolyte NRTL expression, which accounts for the contribution due to short-range interaction forces among all species. The electrolyte NRTL expression was developed based on the NRTL local composition concept, the like ion repulsion assumption, and the local electroneutrality assumption. The like-ion repulsion

assumption stipulates that in the first coordination shell of a cation (anion) the local composition of all other cations (anions) is zero. The local electroneutrality assumption imposes a condition that in the first coordination shell of a molecular species the composition of cations and anion is such that the local electric charge is zero.

The Pitzer-Debye-Hückel expression for excess Gibbs energy, normalized to a mole fraction of unity for the solvent and zero mole fraction for ions, is given as follows:

$$\frac{g^{ex^*,PDH}}{RT} = -\left(\sum_k X_k\right)\left(\frac{1000}{M_s}\right)^{1/2}\left(\frac{4A_\Phi I_x}{\rho}\right)\ln\left(1+\rho I_x^{1/2}\right) \qquad (30)$$

where

$$A_\Phi = \left(\frac{1}{3}\right)\left(\frac{2\pi N_0 d}{1000}\right)^{1/2}\left(\frac{e^2}{DkT}\right)^{2/3}$$

$$I_x = \frac{1}{2}\sum_i Z_i^2 x_i$$

The Born expression for excess Gibbs energy is given as follows:

$$\frac{g^{ex^*,Born}}{RT} = \frac{e^2}{2kT}\left(\frac{1}{D}-\frac{1}{D_w}\right)^{1/2}\left(\sum_i \frac{x_i Z_i^2}{r_i}\right)*10^{-2} \qquad (31)$$

where D stands for the dielectric constant of the solvent mixture with the same solvent ratio as that in the electrolyte solution. D is a function of the temperature, $D_i(T) = A_i + B_i\left[\left(\frac{1}{T}\right)-\left(\frac{1}{C_i}\right)\right]$ and its parameters are found in Aspen Databank [16].

The local-composition electrolyte NRTL expression for excess Gibbs energy is given as follows:

$$g^{ex,lc} = \sum_m X_m \frac{\sum_j X_j G_{jm}\tau_{jm}}{\sum_k X_k G_{km}} + \sum_c X_c \sum_{a'}\left(\frac{X_{a'}}{\sum_{a''} X_{a''}}\right)$$
$$\frac{\sum_j X_j G_{jc,a'c}\alpha_{jc,a'c}}{\sum_k X_k G_{kc,a'c}} + \sum_a X_a \sum_{c'}\left(\frac{X_{c'}}{\sum_{c''} X_{c''}}\right)\frac{\sum_j X_j G_{ja,c'a}\alpha_{ja,c'a}}{\sum_k X_k G_{ka,c'a}} \qquad (32)$$

where

$$G_{jm} = \exp(-\alpha_{jm}\tau_{jm})$$

$$G_{jc,ac} = \exp(-\alpha_{jc,ac}\tau_{jc,ac})$$

$$G_{ja,ca} = \exp(-\alpha_{ja,ca}\tau_{ja,ca}$$

$$G_{cm} = \frac{\sum_a X_a G_{ca,m}}{\sum_{a'} X_{a'}}$$

$$\alpha_{cm} = \frac{\sum_a X_a \alpha_{ca,m}}{\sum_{c'} X_{c'}}$$

$$\alpha_{am} = \frac{\sum_c X_c \alpha_{ca,m}}{\sum_{c'} X_{c'}}$$

$$\tau_{mc,ac} = \tau_{cm} - \tau_{ca,m} + \tau_{m,ca}$$

$$\tau_{ma,ca} = \tau_{am} - \tau_{ca,m} + \tau_{m,ca}$$

The variables τ_{cm} and τ_{am} are computed accordingly from G_{cm} and G_{am}. It is worth mentioning that the first term on the right-hand side of eq 33 represents the short-range interaction contribution where the molecular species are the local center and the second and third terms account for the short-range interaction contributions where cations and anions are the local center, respectively.

In NRTL model, the binary interaction parameters for molecule-molecule binary, molecule-electrolyte binary, and electrolyte-electrolyte binary systems are required for liquid phase activity coefficients calculations. Here, electrolytes are defined as cation and anion pairs.

We set all molecule-molecule and electrolyte-electrolyte binary parameters to zero, unless specified otherwise, and molecule-electrolyte binary parameters to 8 and -4 as reported in NRTL model [12]. The non randomness factor (α) is fixed at 0.2, but it can be variable from 0.1 to 0.9. The calculated thermodynamic properties of the electrolyte solution are dominated by the binary NRTL parameters associated with the major species in the system. The calculated thermodynamic properties of the electrolyte solution are dominated by the binary NRTL parameters associated with the major species in the system. In other words, the binary parameters for the water-MDEA binary, the water-($MDEAH^+$, HCO_3^-) binary, the water-($MDEAH^+$, CO_3^{2-}) binary and the MDEA-($MDEAH^+$, HCO_3^-) binary systems determine the calculated thermodynamic properties. These binary parameters, in turn, are identified from fitting to available experimental data.

After proper consideration of unsymmetrical convention for the solutes and ionic species, the complete excess Gibbs energy expression of the electrolyte NRTL model is given as follows:

$$g^{ex*} = g^{ex,PDH} + g^{ex^*,Born} + g^{ex^*,lc}$$

The activity coefficient for any species *i*, ionic or molecular, solute or solvent, is derived from the partial derivative of the excess Gibbs energy with respect to the mole number of species *i*:

$$\ln\gamma_i = \frac{1}{RT}\left[\frac{\partial(n_i g^{ex*})}{\partial n_i}\right]_{T,P,n_{i\neq j}} \qquad (34)$$

where n_t is the total mole number for all species in the system.

Data regression

At first all available experimental data from different authors were used for regression analysis to obtain the interaction parameters, which resulted in a large average correlation deviation. Then a lot of equilibrium curves were made at the same temperatures and the same initial amine concentrations but from the different authors and some sets of data, which were far away from most of the data, were discarded. Finally, the combination of data useful for generating a correlation to obtain a set of interaction parameters has been identified. The adjustable interaction parameters are characteristic of pair interactions of components of the solution and are independent of solution composition.

Differential evolution algorithm

DE is a stochastic, population-based method [29]. These methods

heuristically "mimic" biological evolution, namely, the process of natural selection and the "survival of the fittest" principle.

Differential evolution (DE) technique is used to estimate the interaction parameters for the VLE model. An adaptive search procedure based on a "population" of candidate solution points is used. "NP" denotes the population size. In a population of potential solutions within an n-dimensional search space, a fixed number of vectors are randomly initialized, then evolved over time to explore the search space and to locate the minima of the objective function. "D" denotes the dimension of each vector, which is actually the number of optimum parameters to be estimated of the proposed objective function ψ (Eq 36)

$$\psi = \sum_{\Delta}^{\Delta i=1 c} \sum_{\Delta}^{\Delta j=1 n} \left| \frac{P_{CO2}^{cal} - P_{CO2}^{\exp}}{P_{CO2}^{\exp}} \right|^2$$

n is the number of experimental data, and c is the number of components in the mixture, respectively.

The main operation in DE is the NP number of competitions, which are to be carried out to decide the next generation population. Generations or iterations involve a competitive selection that drops the poorer solutions. From the current generation population of the vectors, one target vector is selected. Among the remaining population vectors, DE adds the weighted weight factor is denoted by F, and is specified at the starting) difference between two randomly chosen population vectors to third vector, called trial vector (randomly chosen), which results in a "noisy" random vector. This operation is called recombination (mutation). Subsequently, crossover is performed between the trial vector and the noisy random vector (perturbed trial vector) to decide upon the final trial vector or offspring of this generation. For mutation and crossover to be carried out together, a random number is generated which is less than the CR crossover constant). If the random number generated is greater than CR, then the vector taken for mutation (trial vector) is kept copied as it is; as an offspring of this generation (mutation is not compulsory). This way no separate probability distribution has been used which makes the scheme completely self-organizing. Finally, the trial vector replaces the target vector for the next generation population, if and only if it yields a reduced value the objective function than in comparison to the objective function based on target vector. In this way, all the NP number of vectors of the current generation is selected one by one as target vectors and checked whether the trial vector (offspring) to create the population of the next generation should replace them or not. The control parameters of the algorithm are: number of parents (NP), weighing factor or mutation constant (F), crossover constant (CR). There is always a convergence speed (lower F value) and robustness (higher NP value) trade-off. CR is more like a fine tuning element. High values of CR like CR = 1 give faster convergence if convergence occurs.

For each individual $x_{i,G}$ in the current generation G, DE generates a new trial individual $x'_{i,G}$ by adding the weighted difference between two randomly selected individuals $x_{r1,G}$ and $x_{r2,G}$ to a third randomly selected individual $x_{r3,G}$. The resulting individual $x'_{i,G}$ is crossed-over with the original individual, $x_{i,G}$. The fitness of the resulting individual, referred to as perturbated vector $u_{i,G+1}$, is then compared with the fitness of $x_{i,G}$. If the fitness of $u_{i,G+1}$ is greater than the fitness of $x_{i,G}$, $x_{i,G}$ is replaced with $u_{i,G+1}$, otherwise $x_{i,G}$, remains in the population as $u_{i,G+1}$. Deferential Evolution is robust, fast and effective with global optimization ability. It does not require that the objective function is differentiable, and it works with noisy, epistatic and time-dependent objective functions. Pseudocode of DE shows:

$Input: D, G_{\max}, NP4 \geq 4, F \in (0,1+),$

1. $CR \in [0,1], and initial bounds \vec{x}^{(lo)}, \vec{x}^{(hi)}$

$Initialise: \forall i \leq NP \forall j \leq D: x_{i,J,G=0}$

2. $= \vec{x}^{(lo)} + rand_j[0,1] \bullet \left(\vec{x}^{(hi)}, \vec{x}^{(lo)} \right)$

$i=\{1,2,\ldots,NP\},\{1,2,\ldots,D\},$G=0, $rand_i$ [0,1] ∈ [0,1]

3. $While G < G_{\max}$

$\forall i \leq NP$ 4.$MutateandRecombine$

$4.1 r_1, r_2, r_3 \in 1,2,\ldots,NP],$ $randomlyselected, except: r_1 \neq r_2$

$4.2\ j_{rand} \in 1,2,\ldots,D], randomlyselectedonceeachi$

$4.3 \forall_j \leq D, u_{j,i,G+1} = \{x_{j,r3,G} + F.(x_{j,r1,G} - x_{j,r2,G})$

$x_{j,i,G}\ otherwise$

5. Selected i $f\left(rand_j[0,1] < CR \vee j = j_{rand}\right)$

$x_{i,G+1} = \left\{ \vec{u}_{i,G+1}\ iff\left(\vec{u}_{i,G+1}\right) \leq f\left(\vec{u}_{i,G}\right) \right.$

$\{x_{i,G}\ otherwise$

$G = G+1$

There are some versions for optimization by mean differential evolution and two standard versions of DE, one of them, DER and1Bin, are chosen for optimization of eNRTL parameters.

It is recommended to set the number of parents NP to 10 times the number of parameters (eg. For a binary mixtures such as MDEA-H2O, we need two interaction parameters $\tau_{MDEA,H2O} and \tau_{H2O,MDEA}$, then NP should be equal to 20 in this special case), to select weighting factor F=0.8, and crossover constant CR=0.9. It has been found recently that selecting F from the interval [0.5, 1.0] randomly for each generation or for each difference vector, a technique called dither, improves convergence behavior significantly, especially for noisy objective functions. It has also been found that setting CR to a low value, e.g. CR=0.2 helps optimizing separable functions since it fosters the search along the coordinate axes. On the contrary this choice is not effective if parameter dependence is encountered, something which is frequently occurring in real-world optimization problems rather than artificial test functions. So for parameter dependence the choice of CR=0.9 is more appropriate. Another interesting empirical finding is that raising NP above, say, 40 do not substantially improve the convergence, independent of the number of parameters. Different problems often require different settings for NP, F and CR.

Parameter	*i*	*j*	*Value*	*σ(eNRTL-DE)*	*σ(eNRTL-LM)*	*σ(eNRTL-SA)*
a_{ij}	MDEA	H_2O	-1.3781	0.0129	0.0566	0.1472
a_{ji}	H_2O	MDEA	12.153	0.0469	0.1641	0.1078
b_{ij}	MDEA	H_2O	-316.46	5.3898	22.97	10.378
b_{ji}	H_2O	MDEA	-1237.9	8.7256	45.70	9.6247
a_{ij}	CO_2	H_2O	10.064*	-	-	-
a_{ji}	H_2O	CO_2	10.064*	-	-	-
b_{ij}	CO_2	H_2O	-3268.135*	-	-	-
b_{ji}	H_2O	CO_2	-3268.135	-	-	-

Table 2: eNRTL parameters τ) for the MDEA-H_2O using Differential Evolution Algorithm (α = 0.2). $\hat{o} = a + \frac{b}{T}$, where T is the temperature in K and σ is the standard deviation.

Parameter	*i*	*j*	*Value*	σ
τ_{ij}	H2O	(MDEAH+, HCO_3^-)	6.2699	0.0981
τ_{ji}	(MDEAH+, HCO_3^-)	H2O	-7.8856	0.0194
τ_{ij}	H2O	(MDEAH+, CO_3^{2-})	17.2754	0.0367
τ_{ji}	(MDEAH+, CO_3^{2-})	H2O	-0.1982	0.0653
τ_{ij}	MDEA	(MDEAH+, HCO_3^-)	11.3765	0.0762
τ_{ji}	(MDEAH+, HCO_3^-)	MDEA	-3.1299	0.0492

Table 3: eNRTL parameters molecule-electrolyte binaries (τ) for the MDEA-H_2O-CO_2 system with DE (α = 0.2).

The strategy adopted

Different strategies can be adopted in DE algorithm depending upon the type of problem for which DE is applied. The strategies can vary; based on the vector to be perturbed, number of difference vectors considered for perturbation, and finally the type of crossover used [28].

The DE algorithm is a population based algorithm like genetic algorithms using the similar operators; crossover, mutation and selection. The main difference in constructing better solutions is that genetic algorithms rely on crossover while DE relies on mutation operation. This main operation is based on the differences of randomly sampled pairs of solutions in the population.

The algorithm uses mutation operation as a search mechanism and selection operation to direct the search toward the prospective regions in the search space. The DE algorithm also uses a non-uniform crossover that can take child vector parameters from one parent more often than it does from others. By using the components of the existing population members to construct trial vectors, the recombination

Parameters	**Component**	**Source**	**Type of Data required in regression and their sources**
$\Delta_f G_{298.15}^{ig}$	H2O, MDEA, CO2	Aspen Databank [16]	
$\Delta_f H_{298.15}^{ig}$	H2O, MDEA, CO2	Aspen Databank [16]	
O_3^-	H2O, CO2 MDEA	Aspen Databank [16] **Regression**	**Data** (Liquid heat capacity of MDEA) **Regression** (Maham et al. [35], Chen et al. [34], Zhang et al. [35])
$\Delta_{f_{CO_2(v)\leftrightarrow CO_2(l)}}$	H_3O^+, OH^-, HCO_3^-, CO_3^{2-} $MDEAH^+$	Aspen Databank [16] **Regression**	**Data** (VLE, excess enthalpy, heat capacity, and species concentration from NMR spectra for the MDEA-H_2O-CO_2 system) **Regression** (Kuranov et al. [36], Kamps et al. [37], Ermatchkov et al. [13], Mathonat [39], Weiland et al. [40], Jackobsen et al. [41])
$\Delta_f H_{298.15}^{\infty,aq}$	H_3O^+, OH^-, HCO_3^-, CO_3^{2-} $MDEAH^+$	Aspen Databank [16] **Regression**	**Data** (VLE, excess enthalpy, heat capacity, and species concentration from NMR spectra for the MDEA-H_2O-CO_2 system) **Regression** (Kuranov et al. [36], Kamps et al. [37], Ermatchkov et al. [38], Mathonat [39], Weiland et al. [40], Jackobsen et al. [41])
$C_P^{\infty,aq}$	H_3O^+, OH^-	Aspen Databank [16] Criss and Cobble [31] **Regression**	**Data** (VLE, excess enthalpy, heat capacity, and species concentration from NMR spectra for the MDEA-H_2O-CO_2 system) **Regression** (Kuranov et al. [36], Kamps et al. [37], Ermatchkov et al. [38], Mathonat [39], Weiland et al. [40], Jackobsen et al. [41])
$\Delta_{vap}H$	MDEA	**Regression**	Heat of vaporization of MDEA, calculated from the vapor Pressure (Antoine Equation) using the Clausius-Clapeyron equation
Antoine Equation	MDEA	**Regression**	**Data** (Vapor pressure of MDEA, heat of vaporization of MDEA, calculated from the vapor pressure using the Clausius-Clapeyron equation) **Regression** (Daubert et al. [42], Noll et al. [43], VonNiederhausern et al. [44])
Dielectric Constant	MDEA	Criss and Cobble [31]	
Henry's Constant	CO2 in H2O CO2 in MDEA	Yan and Chen [32] Zhang & Chen [33]	
NRTL-Electrolyte Binary Parameters	CO2-H2O binary MDEA-H2O binary MDEA-H2O-CO2 Molecule-Electrolyte Binaries	**Regression$^{1\text{-DE}}$** **Regression$^{2\text{-DE}}$** **Regression$^{3\text{-DE}}$**	**Data** 1. Solubility of CO2 in pure water 2. VLE, excess enthalpy, and heat capacity for the MDEA-H_2O and CO_2-H_2O binaries 3. VLE, excess enthalpy, heat capacity, and species concentration from NMR spectra for the MDEA-H_2O-CO_2 system **Regression** 1. Yan & Chen [32] 2. (Xu et al. [45], Voutsas et al. [46], Kim et al. [47], Posey [9], Maham et al. [30,31], Chiu and Li [48], Chen e al. [50], Zhang et al. [49]) 3. (Kuranov et al. [36], Kamps et al. [37], Ermatchkov et al. [38], Mathonat [39], Weiland et al. [40], Jackobsen et al. [41])

Table 4: Parameters estimated in modelling with their sources and the type of data regressed.

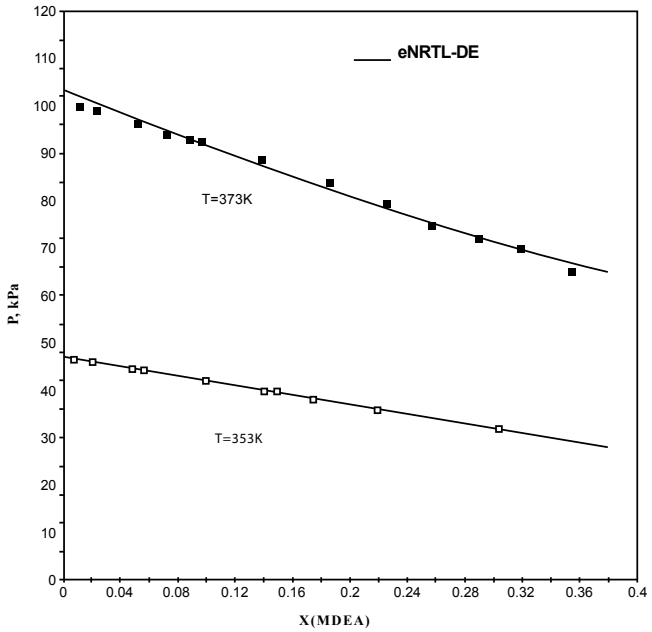

Figure 1: Comparison of the experimental data from Kim et al. [47] with the model eNRTL-DE for MDEA-H_2O system.

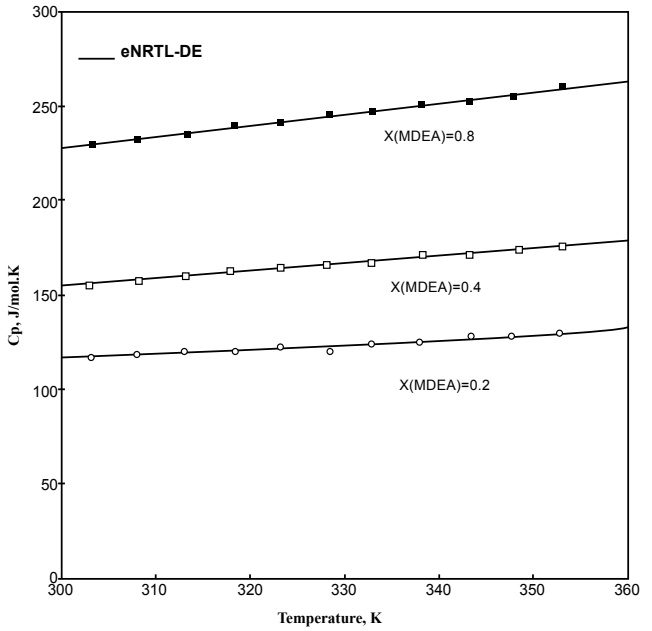

Figure 2: Comparison of the experimental (MDEA-H_2O) data from Chen et al. [1,2] with the model eNRTL-DE for MDEA-H_2O system.

(crossover) operator efficiently shuffles information about successful combinations, enabling the search for a better solution space.

An optimization task consisting of D parameters can be represented by a D-dimensional vector. In DE, a population of NP solution vectors is randomly created at the start. This population is successfully improved by applying mutation, crossover and selection operators. The main steps of the DE algorithm are given below:

- **Initialization**
- **Evaluation**
- **Repeat**

Mutation

Recombination

Evaluation

Selection

- **Until** (termination criteria are met)

Results and Discussions

Only, the eNRTL parameters (Tables 2 and 3) have been regressed

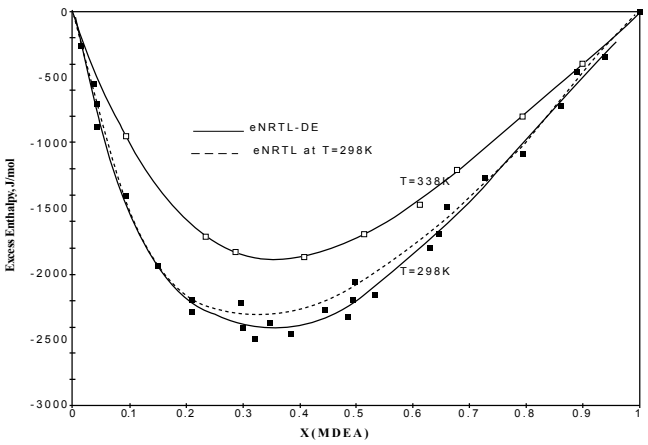

Figure 3: Comparison of the experimental data from Posey with the model eNRTL-DE for MDEA-H_2O. For comparison eNRTL is also represented.

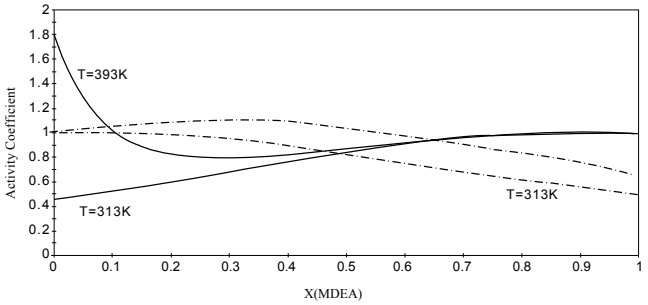

Figure 4: Model predictions of MDEA and H_2O activity coefficients: (_____) H_2O activity coefficients and (-.-.-.-) MDEA activity coefficients.

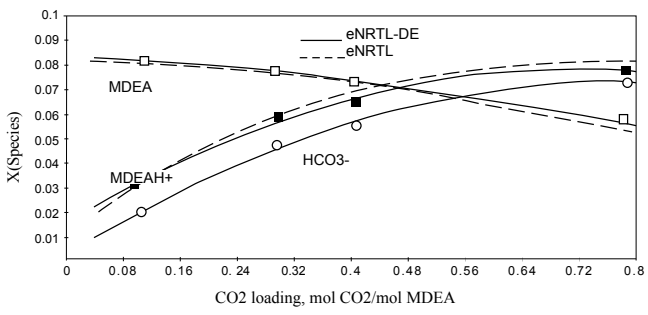

Figure 5: Comparison of the experimental data for some species concentration in MDEA-CO_2-H_2O system at T=293K and MDEA concentration 23 wt%. For comparison eNRTL is also represented.

using differential evolution algorithm, the rest of the data have been taken from the literature. Table 4 summarizes the model parameters and sources of the parameters used in the thermodynamic model. Most of the parameters can be obtained from the literature. A lot of results can be plotted but we confined ourselves a few of them to show the modeling compared to the experimental and sometimes compared to eNRTL without DE algorithm. Figure 1 shows the comparison for the experimental total pressure data and the calculated results from the model. Figure 1 shows the model also provides excellent representation of the heat capacity data.

The excess enthalpy fit is given in Figure 3. Both the experimental excess enthalpy data from Posey [4] and those of Maham et al. [35,43] are represented very well. It shows also a better fit for eNRTL-DE model. Figure 4 shows the model predictions for water and MDEA activity coefficients at 313, 353, and 393°K. While the water activity coefficient remains relatively constant, the model suggests that the MDEA activity coefficient varies strongly with MDEA concentration and temperature, especially in dilute aqueous MDEA solutions.

Figure 5 shows the species distribution as a function of CO_2 loading for a 23 wt% MDEA solution at 293°K. The calculated concentrations of the species are consistent with the experimental NMR measurements from Jakobsen et al. [41].

Figures 6 show comparisons of the model correlations and the experimental data of Mathonat 65 for the integral heat of CO_2 absorption in aqueous MDEA solution at 313°K. The calculated values are in good agreement with the experimental data. Also shown in Figure 6 are the predicted differential heats of CO_2 absorption.

Table 4 summarizes the model parameters, sources of the parameters and the type of data used in the thermodynamic model. Most of the parameters can be obtained from the literature. The remaining parameters are determined by fitting to the experimental data. For MDEA-H_2O binary only, the standard deviations are compared using DE algorithm and Levenberg–Marquardt (LM) algorithms (Table 2). It is clear that DE presents lower σ than LM and SA.

Conclusions

The electrolyte eNRTL model has been successfully applied with Differential Evolution algorithm to calculate the interaction parameters and to correlate the experimental data on thermodynamic properties of MDEA-H_2O-CO_2 system. The model has validated a lot of experimental data, but more research needs to be carrying out to compare eNRTL-DE with eNRTL-LM and eNRTL-LM for all the interactions parameters. The model can be used to support process modeling and simulation of the CO_2 capture process with MDE.

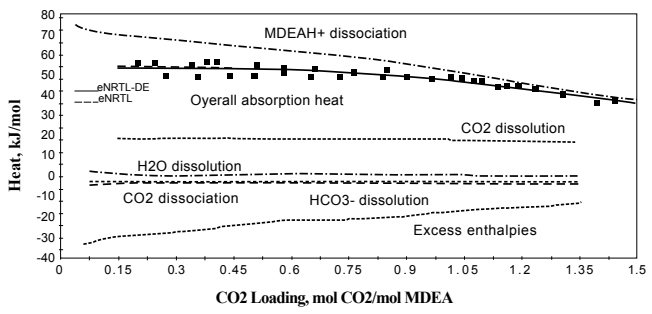

Figure 6: Heat of reaction of the different components in 30 wt% MDEA solution at T=313K.

References

1. Chen CC, Mathias PM (2002) Applied Thermodynamics for Process Modeling. AIChE J 48: 194–200.
2. Chen CC (2006) Toward Development of Activity Coefficient Models for Process and Product Design of Complex Chemical Systems. Fluid Phase Equilib 241: 103–112.
3. Austgen DM, Rochelle GT, Chen CC (1991) Model of Vapor- Liquid Equilibria for Aqueous Acid Gas-Alkanolamine Systems. 2. Representation of H2S and CO2 Solubility in Aqueous MDEA and CO2 Solubility in Aqueous Mixtures of MDEA with MEA or DEA. Ind Eng Chem Res 30: 543–555.
4. Posey ML (1996) Thermodynamic Model for Acid Gas Loaded Aqueous Alkanolamine Solutions. PhD dissertation, The University of Texas at Austin, USA.
5. Song Y, Chen CC (2009) Symmetric Electrolyte Nonrandom Two- Liquid Activity Coefficient Model. Ind Eng Chem Res 48: 7788– 7797.
6. Chen CC, Evans LB (1986) A Local Composition Model for the Excess Gibbs Energy of Aqueous Electrolyte Systems. AIChE J 32: 444–454.
7. Chen CC, Britt HI, Boston JF, Evans LB (1982) Local Composition Model for Excess Gibbs Energy of Electrolyte Systems. Part I: Single Solvent, Single Completely Dissociated Electrolyte Systems. AIChE J 28: 588–596.
8. Kuranov G, Rumpf B, Smirnova NA, Maurer G (1996) Solubility of Single Gases Carbon Dioxide and Hydrogen Sulfide in Aqueous Solutions of *N*-Methyldiethanolamine in the Temperature Range 313-413 K at Pressures up to 5 MPa. Ind Eng Chem Res 35: 1959–1966.
9. Kamps APS, Balaban A, Jodecke M, Kuranov G, Smirnova NA, Maurer G (2001) Solubility of Single Gases Carbon Dioxide and Hydrogen Sulfide in Aqueous Solutions of *N*-Methyldiethanolamine at Temperatures from 313 to 393 K and Pressures up to 7.6 MPa: New Experimental Data and Model Extension. Ind Eng Chem Res 40: 696–706.
10. Faramarzi L, Kontogeorgis GM, Thomsen K, Stenby EH (2009) Extended UNIQUAC Model for Thermodynamic Modeling of CO2 Absorption in Aqueous Alkanolamine Solutions. Fluid Phase Equilib 282: 121–132.
11. Thomsen K, Rasmussen P (1999) Modeling of Vapor-Liquid-Solid Equilibrium in Gas-Aqueous Electrolyte Systems. Chem Eng Sci 54: 1787–1802.
12. Arcis H., Rodier L, Karine BB, Coxam JY (2009) Modeling of (Vapor + Liquid) Equilibrium and Enthalpy of Solution of Carbon Dioxide (CO2) in Aqueous Methyldiethanolamine (MDEA) Solutions. J Chem Thermodyn 41: 783–789.
13. Storn R, Price K (1997) Differential evolution - a simple and efficient heuristic for global optimization over continuous spaces. Journal of Global Optimization 11: 341–359.
14. Gross J, Sadowski G (2001) Perturbed-Chain SAFT: An Equation of State Based on a Perturbation Theory for Chain Molecules. Ind Eng Chem Res 40: 1244–1260.
15. Gross J, Sadowski G (2002) Application of the Perturbed-Chain SAFT Equation of State to Associating Systems. Ind Eng Chem Res 41: 5510–5515.
16. Aspen Physical Property System, V7.2; Aspen Technology, Inc.: Burlington, MA, 2010.
17. Van Ness HC, Abbott MM (1979) Vapor-Liquid Equilibrium: Part VI. Standard State Fugacities for Supercritical Components. AIChE J 25: 645–653.
18. Brelvi SW, O'Connell JP (1972) Corresponding States Correlations for Liquid Compressibility and Partial Molar Volumes of Gases at Infinite Dilution in Liquids. AIChE J 18: 1239–1243.
19. Yan YZ, Chen CC (2010) Thermodynamic Modeling of CO2 Solubility in Aqueous Solutions of NaCl and Na2SO4. J Supercrit Fluids 55: 623-634.
20. Wang YW, Xu S, Otto FD, Mather AE (1992) Solubility of N2O in Alkanolamines and in Mixed Solvents. Chem Eng J 48: 31–40.

21. Versteeg GF, Van Swaaij WPM (1998) Solubility and Diffusivity of Acid Gases (CO2, N2O) in Aqueous Alkanolamine Solutions. J Chem Eng Data 33: 29–34.

22. Wagman DD, Evans WH, Parker VB, Schumm RH, Halow I, Bailey SM, Churney KL, Nuttall RL (1982) The NBS tables of chemical thermodynamic properties. Selected values for inorganic and C1 and C2 organic substances in SI units. J Phys Chem Ref 11: 2-38 and 2-83.

23. Criss CM, Cobble JW (1964) The Thermodynamic Properties of High Temperature Aqueous Solutions. V. The Calculation of Ionic Heat Capacities up to 2C0°. Entropies and Heat Capacities above 200°. J Am Chem Soc 86: 5390–5393.

24. Kamps APS, Maurer G (1996) Dissociation Constant of *N*-Methyldiethanolamine in Aqueous Solution at Temperatures from 278 to 368 K. J Chem Eng Data 41: 505–1513.

25. Von Niederhausern DM, Wilson GM, Giles NF (2006) Critical Point and Vapor Pressure Measurements for 17 Compounds by a Low Residence Time Flow Method. J Chem Eng Data 51: 1990–1995.

26. Daubert TE, Hutchison G (1990) Vapor Pressure of 18 Pure Industrial Chemicals. AIChE Symp Ser 86: 93–114.

27. Noll O, Valtz A, Richon D, Getachew-Sawaya T, Mokbel I (1998) Vapor Pressures and Liquid Densities of *N*-Methylethanolamine, Diethanolamine, and *N*-Methyldiethanolamine. ELDATA: Int Electron J Phys Chem Data 4: 105–120.

28. Babu BV (2004) Process Plant Simulation. Oxford University Press, New Delhi, India.

29. Storn R (1997) J Global Optim 11: 341.

30. Maham Y, Mather AE, Hepler LG (1997) Excess Molar Enthalpies of (Water + Alkanolamine) Systems and Some Thermodynamic Calculations. J Chem Eng Data 42: 988–992.

31. Maham Y, Mather AE, Mathonat C (2000) Excess properties of (alkyldiethanolamine + H_2O) mixtures at temperatures from (298.15 to 338.15) K. J Chem Thermodyn 32: 229–236.

32. Yan YZ, Chen CC (2010) Thermodynamic Modeling of CO_2 Solubility in Aqueous Solutions of NaCl and Na_2SO_4. J Supercrit Fluids 55: 623-634.

33. Zhang Y, Chen CC (2011) Thermodynamic Modeling for CO_2 Absorption in Aqueous MDEA Solution with Electrolyte NRTL Model. Ind Eng Chem Res 50: 163–175.

34. Chen YJ, Shih TW, Li MH (2001) Heat Capacity of Aqueous Mixtures of Monoethanolamine with *N*-Methyldiethanolamine. J Chem Eng Data 46: 51–55.

35. Zhang K, Hawrylak B, Palepu R, Tremaine PR (2002) Thermodynamics of Aqueous Amines: Excess Molar Heat Capacities, Volumes, and Expansibilities of (Water + Methyldiethanolamine (MDEA)) and (Water + 2-Amino-2-methyl-1-propanol (AMP)). J Chem Thermodyn 34: 679–710.

36. Kuranov G, Rumpf B, Smirnova NA, Maurer G (1996) Solubility of Single Gases Carbon Dioxide and Hydrogen Sulfide in Aqueous Solutions of *N*-Methyldiethanolamine in the Temperature Range 313-413 K at Pressures up to 5 MPa. Ind Eng Chem Res 35: 1959-1966.

37. Kamps APS, Balaban A, Jödecke M, Kuranov G, Smirnova NA, et al. (2001) Solubility of Single Gases Carbon Dioxide and Hydrogen Sulfide in Aqueous Solutions of N-Methyldiethanolamine at Temperatures from 313 to 393 K and Pressures up to 7.6 MPa: New Experimental Data and Model Extension. Ind Eng Chem Res 40: 696-706.

38. Ermatchkov V, Kamps APS, Maurer G (2006) Solubility of Carbon Dioxide in Aqueous Solutions of *N* Methyldiethanolamine in the Low Gas Loading Region. Ind Eng Chem Res 45: 6081-6091.

39. Mathonat C, Grolier JPE (1995) Calorimetrie de me´lange, a ecoulement, a temperatures et pressions elevees. Application a l'etude de l'elimination du dioxide de carbone a l'aide de solutions aqueuses d'alcanolamines. Universite Blaise Pascal Paris p 265.

40. Weiland RH, Dingman JC (1997) Cronin DB Heat capacity of Aqueous Monoethanolamine, Diethanolamine, N-Methyldiethanolamine, and *N*-Methyldiethanolamine-Based Blends with Carbon Dioxide. J Chem Eng Data 42: 1004-1006.

41. Jakobsen JP, Krane J, Svendsen HF (2005) Liquid-Phase Composition Determination in CO2-H2O-Alkanolamine Systems: An NMR Study. Ind Eng Chem Res 44: 9894-9903.

42. Daubert T E, Hutchison G (1990) Vapor Pressure of 18 Pure Industrial Chemicals. AIChE Symp Ser 86: 93-114.

43. Noll O, Valtz A, Richon D, Getachew-Sawaya T, Mokbel I, et al. (1998) Vapor Pressures and Liquid Densities of N-Methylethanolamine, Diethanolamine, and N-Methyldiethanolamine. ELDATA: Int Electron J Phys Chem Data 4: 105-120.

44. Von Niederhausern DM, Wilson GM, Giles NF (2006) Critical Point and Vapor Pressure Measurements for 17 Compounds by a Low Residence Time Flow Method. J Chem Eng Data 51: 1990-1995.

45. Xu S, Qing S, Zhen Z, Zhang C, Carroll J (1991) Vapor Pressure Measurements of Aqueous N-Methyldiethanolamine Solutions. Fluid Phase Equilib 67: 197-201.

46. Voutsas E, Vrachnos A, Magoulas K (2004) Measurement and Thermodynamic Modeling of the Phase Equilibrium of Aqueous N-Methyldiethanolamine Solutions. Fluid Phase Equilib 224: 193-197.

47. Kim I, Svendsen HF, Børresen E (2008) Ebulliometric Determination of Vapor-Liquid Equilibria for Pure Water, Monoethanolamine, *N*-Methyldiethanolamine, 3-(Methylamino)-propylamine and Their Binary and Ternary Solutions. J Chem Eng Data 53: 2521-2531.

48. Chiu LF, Li MH (1999) Heat Capacity of Alkanolamine Aqueous Solutions. J Chem Eng Data 44: 1396–1401.

49. Zhang K, Hawrylak B, Palepu R, Tremaine PR (2002) Thermodynamics of Aqueous Amines: Excess Molar Heat Capacities, Volumes, and Expansibilities of (Water + Methyldiethanolamine (MDEA)) and (Water + 2-Amino-2-methyl-1-propanol (AMP)). J Chem Thermodyn 34: 679–710.

50. Chen YJ, Shih TW, Li MH (2001) Heat Capacity of Aqueous Mixtures of Monoethanolamine with *N*-Methyldiethanolamine. J Chem Eng Data 46: 51–55.